

**MATHEMATICAL ANALYSIS OF
HERSCHEL-BULKLEY FLUID MODEL
FOR SOLUTE DISPERSION IN BLOOD FLOW
THROUGH NARROW CONDUITS**

NURUL AINI BINTI JAAFAR

UNIVERSITI SAINS MALAYSIA

2017

**MATHEMATICAL ANALYSIS OF
HERSCHEL-BULKLEY FLUID MODEL
FOR SOLUTE DISPERSION IN BLOOD FLOW
THROUGH NARROW CONDUITS**

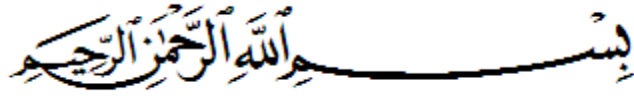
by

NURUL AINI BINTI JAAFAR

**Thesis submitted in fulfillment of the requirements
for the degree of
Doctor of Philosophy**

February 2017

ACKNOWLEDGEMENT



In the name of Allah, the Entirely Merciful, the Especially Merciful

First and foremost, thanks to Almighty Allah Subhanahu wa Ta'ala for graciously bestowing me the strength to complete this thesis. I would like to express my heartfelt gratitude to my main supervisor, Dr. Yazariah Mohd Yatim and also to my field supervisor, Prof. Duraisamy Sambasivam Sankar from Engineering Mathematics Unit, Universiti Teknologi Brunei for their guidance, encouragement, advice, patience and full support to me in completing this thesis successfully. Their time and effort spent for this thesis are precious. I have learned many valuable lessons from them.

I would like to express my thanks to my beloved husband, my dearest parents and family for their love, prayer and support during my toughest time. Also, thanks a lot to my friends and labmates for their help and friendship during all these years. I sincerely thank the ministry of Higher Education for providing the MyBrain15 financial support for my PhD program. I also thank the technical and academic staffs of School of Mathematical Sciences, USM for providing me the research facilities during the preparation of this thesis. Lastly, I thank all who helped me directly or indirectly in completing the thesis.

TABLE OF CONTENTS

Acknowledgement	ii
Table of Contents	iii
List of Tables	xi
List of Figures	xii
List of Abbreviations	xvii
List of Symbols	xviii
Abstrak	xxv
Abstract	xxvii

CHAPTER 1 – INTRODUCTION

1.1 Background of Study	1
1.2 Cardiovascular System.....	5
1.2.1 The blood vessels	6
1.2.2 The heart	9
1.2.3 The blood	10
1.2.3(a) The constituents of blood	10
1.2.3(b) Blood rheology	11
1.3 The Fluid Models	12
1.3.1 Newtonian fluid model.....	14
1.3.2 Non-Newtonian fluid models.....	15
1.3.2(a) Power-law fluid model	15
1.3.2(b) Bingham plastic fluid model	16
1.3.2(c) Casson fluid model	16
1.3.2(d) Herschel-Bulkley (H-B) fluid model.....	17

1.3.2(e) The advantages of Herschel-Bulkley (H-B) fluid	18
1.4 Basic Concepts of Fluid Mechanics.....	19
1.4.1 Cartesian and cylindrical coordinate systems	21
1.4.2 Types of flow	22
1.4.2(a) Steady and unsteady flows	22
1.4.2(b) Laminar and turbulent flows	22
1.4.2(c) Incompressible and compressible flows	23
1.4.2(d) Fully-developed flow	23
1.4.2(e) Plane Poiseuille flow	24
1.4.2(f) Hagen-Poiseuille flow	25
1.4.2(g) Uniform and non-uniform flows	26
1.4.3 Governing equations	26
1.4.3(a) Equation of continuity	27
1.4.3(b) Equation of momentum (Navier-Stokes)	29
1.4.4 Dimensional analysis	33
1.5 Basic Concepts of Convective-Diffusion Equation	33
1.5.1 Dispersion	34
1.5.2 Convection	34
1.5.3 Diffusion	37
1.5.4 Derivation of convective-diffusion equation	38
1.5.5 Physical interpretation of the dimensionless numbers and parameters.....	41
1.5.5(a) Péclet number	41
1.5.5(b) Damköhler number.....	42
1.5.5(c) Chemical reaction rate parameter	43
1.5.5(d) Wall absorption parameter	43

1.6 Issues and Gaps of Study	44
1.7 Problem Statement	46
1.8 Objectives and Scopes of Study	47
1.9 Limitations of Study	48
1.10 Contributions of Study	49
1.11 Outline of Thesis	50

CHAPTER 2 – LITERATURE REVIEW

2.1 Introduction	52
2.2 Literature Survey on the Solute Dispersion	52
2.2.1 The unsteady dispersion of solute in a Newtonian fluid model.....	52
2.2.2 The unsteady dispersion of solute with the effect of wall absorption in a Newtonian fluid model	56
2.2.3 The steady dispersion of solute in non-Newtonian fluid models.....	58
2.2.4 The unsteady dispersion of solute in non-Newtonian fluid models.....	60
2.2.5 The unsteady dispersion of solute with the effect of irreversible wall absorption in non-Newtonian fluid models.....	63
2.2.6 The unsteady dispersion of solute with the effect of chemical reaction	64
2.2.7 The unsteady dispersion of solute with the effect of irreversible wall absorption and reversible phase exchange	67
2.2.8 The unsteady dispersion of solute in an annulus	69
2.2.9 The steady dispersion of solute in a stenosed artery	70

CHAPTER 3 – STEADY DISPERSION OF SOLUTE IN BLOOD FLOW THROUGH NARROW CONDUITS

3.1 Introduction.....	74
3.2 Mathematical Formulation.....	75
3.2.1 Flow in a circular pipe	76
3.2.1(a) Governing equations.....	76
3.2.1(b) Method of solution	81
3.2.2 Flow in a channel	91
3.2.2(a) Governing equations.....	91
3.2.2(b) Method of solution	94
3.3 Results and Discussions	102
3.3.1 Normalized velocity distribution	103
3.3.2 Non-dimensional effective axial diffusivity	107
3.3.3 Relative axial diffusivity.....	111
3.3.4 Some physiological applications.....	114
3.4 Conclusions.....	117

CHAPTER 4 – STEADY DISPERSION OF SOLUTE IN BLOOD FLOW THROUGH NARROW CONDUITS WITH THE EFFECT OF CHEMICAL REACTION

4.1 Introduction.....	119
4.2 Mathematical Formulation.....	121
4.2.1 Flow in a circular pipe	121
4.2.1(a) Governing equations.....	121
4.2.1(b) Method of solution	125
4.2.2 Flow in a channel	127
4.2.2(a) Governing equations.....	127

4.2.2(b) Method of solution	128
4.3 Results and Discussions	130
4.3.1 Non-dimensional effective axial diffusivity	131
4.3.2 Relative axial diffusivity	136
4.3.3 Some physiological applications.....	141
4.4 Conclusions.....	143

CHAPTER 5 – UNSTEADY DISPERSION OF SOLUTE IN BLOOD FLOW THROUGH NARROW CONDUITS WITH THE EFFECT OF CHEMICAL REACTION

5.1 Introduction.....	145
5.2 Mathematical Formulation.....	147
5.2.1 Flow in a circular pipe	148
5.2.1(a) Governing equations.....	148
5.2.1(b) Non-dimensional variables.....	149
5.2.1(c) Method of solution	152
5.2.1(d) Generalized dispersion model	154
5.2.1(e) Governing differential equations and solutions of dispersion function.....	154
5.2.1(f) Solution of longitudinal diffusion coefficient.....	160
5.2.1(g) Solution of mean concentration of solute.....	161
5.2.1(h) Solution of local concentration.....	163
5.2.2 Flow in a channel	164
5.2.2(a) Governing equations.....	164
5.2.2(b) Non-dimensional variables.....	165
5.2.2(c) Method of solution	166
5.2.2(d) Generalized dispersion model	168

5.2.2(e) Governing differential equations and solutions of dispersion function.....	168
5.2.2(f) Solution of longitudinal diffusion coefficient.....	171
5.2.2(g) Solution of mean concentration of solute.....	172
5.2.2(h) Solution of local concentration.....	172
5.3 Results and Discussions	172
5.3.1 Steady dispersion function	173
5.3.2 Unsteady dispersion function.....	179
5.3.3 Dispersion function	186
5.3.4 Longitudinal diffusion coefficient	189
5.3.5 Relative axial diffusivity	193
5.3.6 Mean concentration of solute.....	197
5.4 Conclusions.....	202

CHAPTER 6 – UNSTEADY DISPERSION OF SOLUTE IN BLOOD FLOW THROUGH NARROW CONDUITS WITH THE EFFECT OF REVERSIBLE AND IRREVERSIBLE REACTIONS AT THE WALL

6.1 Introduction.....	204
6.2 Mathematical Formulation.....	207
6.2.1 Flow in a circular pipe	207
6.2.1(a) Governing equations.....	207
6.2.1(b) Non-dimensional variables.....	210
6.2.1(c) Method of solution	212
6.2.1(d) Generalized dispersion model	213
6.2.1(e) Governing differential equations and solutions of dispersion function.....	213

6.2.1(f) Solution of exchange, longitudinal convection and dispersion coefficients	218
6.2.1(g) Steady state of dispersion function, exchange, longitudinal convection and dispersion coefficients.....	218
6.2.1(h) Solution of mean concentration of solute.....	223
6.2.2 Flow in a channel	225
6.2.2(a) Governing equations.....	225
6.2.2(b) Non-dimensional variables.....	227
6.2.2(c) Method of solution	228
6.2.2(d) Generalized dispersion model	228
6.2.2(e) Governing differential equations and solutions of dispersion function.....	229
6.2.2(f) Solution of exchange, longitudinal convection and dispersion coefficients	231
6.2.2(g) Steady state of dispersion function, exchange, longitudinal convection and dispersion coefficients.....	232
6.2.2(h) Solution of mean concentration of solute.....	236
6.3 Results and Discussions	236
6.3.1 Negative asymptotic exchange coefficient	237
6.3.2 Negative asymptotic convection coefficient	240
6.3.3 Asymptotic longitudinal diffusion coefficient	246
6.3.4 Mean concentration of solute.....	252
6.4 Conclusions.....	258

CHAPTER 7 – CONCLUSIONS AND FUTURE WORK

7.1 Conclusions.....	260
7.2 Suggestions for Future Research	264

REFERENCES	266
-------------------------	-----

APPENDICES

Appendix A – The dimensions and derivations of viscosity in Chapter 1

Appendix B – The derivations of velocity and some solutions in Chapter 3

Appendix C – The solutions of \bar{C}_2 , $Y(r_p)$ and $H(x_p)$ in Chapter 4

Appendix D – The derivations of \bar{u}_0 and some solutions in Chapter 5

Appendix E – The solutions of K_1 and K_2 in Chapter 6

LIST OF PUBLICATIONS

LIST OF TABLES

	Page	
Table 3.1	<p>Estimates of the relative axial diffusivity of solute in the canine vascular system in H-B and Casson fluids for (a) flow in a circular pipe (Eq. (3.65)) and (b) flow in a channel (Eq. (3.120)).</p>	115
Table 3.2	<p>Estimates of the effective axial diffusivity of solute in the canine vascular system in H-B and Casson fluids with $Pe = 12$ for (a) flow in a circular pipe (Eq. (3.64)) and (b) flow in a channel (Eq. (3.119)).</p>	117
Table 4.1	<p>Estimates of the relative axial diffusivity of solute in H-B fluid for different values of chemical reaction rate parameter and power-law index at $r_p = x_p = 0.1$ for flow in a circular pipe (Eq. (4.18)) and a channel (Eq. (4.31)).</p>	140
Table 4.2	<p>Estimates of the relative axial diffusivity of solute in the canine vascular system in H-B and Casson fluids with chemical reaction rate parameter $\bar{R} = 10$ for (a) flow in a circular pipe (Eq. (4.18)) and (b) flow in a channel (Eq. (4.31)).</p>	142
Table 5.1	<p>Variation of relative axial diffusivity of solute for H-B fluid model with yield stress for steady dispersion for (a) flow in a circular pipe and (b) flow in a channel.</p>	199
Table 6.1	<p>Variation of negative asymptotic convection coefficient ($-K_1$) with wall absorption parameter β for different values of the power-law index n at $r_p = x_p = 0.1$, Damköhler number $Da = 0.1$ and partition coefficient $\sigma = 0.5$ in H-B fluid for flow in a circular pipe (Eq. (6.76)) and a channel (Eq. (6.153)).</p>	245
Table 6.2	<p>Comparison of the negative asymptotic convection coefficient with wall absorption parameter β for different fluid models with reversible phase exchange and no phase exchange at $r_p = x_p = 0.1$ and $n = 1.05$ for (a) flow in a circular pipe and (b) flow in a channel.</p>	248
Table 6.3	<p>Comparison of the asymptotic longitudinal diffusion coefficient with wall absorption parameter β for different fluid models with reversible and no reversible reaction at yield stress $r_p = x_p = 0.1$ and $n = 1.05$ for (a) flow in a circular pipe and (b) flow in a channel.</p>	256

LIST OF FIGURES

		Page
Figure 1.1	The Wyss Institute's human breathing lung-on-a-chip. It is a microdevice the size of memory stick used for testing drug and toxin (Larkin, 2015).	4
Figure 1.2	A diagram representation of the human cardiovascular system (The human circulatory system, n.d.).	6
Figure 1.3	Structures of the artery, vein, capillary, venule and arteriole (Arteries and veins, n.d.).	8
Figure 1.4	The differences between an artery, a vein and a capillary (The human circulatory system, n.d.).	8
Figure 1.5	The structure of the heart (Boundless, 2015b).	9
Figure 1.6	The relationship between the shear stress and shear rate for Newtonian and certain non-Newtonian fluids.	14
Figure 1.7	Coordinate of the point P for (a) Cartesian and (b) cylindrical coordinate systems (modified from Kay, 1964).	20
Figure 1.8	The development of velocity profile in a circular pipe (modified Cengel & Cimbala, 2006).	23
Figure 1.9	Velocity profile of plane Poiseuille flow.	25
Figure 1.10	Velocity profile of Hagen-Poiseuille flow.	26
Figure 3.1	The geometries of the fluid flow for (a) flow in a circular pipe and (b) flow in a channel.	76
Figure 3.2	Normalized velocity profiles (Eq. (3.33)) with radius r and semi-width x for different values of yield stress r_p and x_p and power-law index n for Newtonian and some non-Newtonian fluids for (a) flow in a circular pipe and (b) flow in a channel.	105
Figure 3.3	Variation of non-dimensional effective axial diffusivity with yield stress r_p and x_p for different values of Péclet number Pe at power-law index $n = 0.95$ and $n = 1.05$ for some non-Newtonian fluids for (a) flow in a circular pipe (Eq. (3.62)) and (b) flow in a channel (Eq. (3.118)).	110
Figure 3.4	Comparison of relative axial diffusivity with yield stress r_p and x_p for different values of power-law index n for some non-Newtonian fluids for flow in a circular pipe (Eq. (3.65)) and a channel (Eq. (3.120)).	113

Figure 3.5	Comparison of relative axial diffusivity with $1/n$ for different values of yield stress r_p and x_p for some non-Newtonian fluids for flow in a circular pipe (Eq. (3.65)) and a channel (Eq. (3.120)).	113
Figure 4.1	The geometries of the fluid flow with chemical reaction for (a) flow in a circular pipe and (b) flow in a channel.	122
Figure 4.2	Variation of effective axial diffusivity with yield stress r_p and x_p for different values of Péclet number Pe at chemical reaction rate parameter $\bar{R} = 10$, power-law index $n = 0.95$ and $n = 1.05$ for H-B and Casson fluids for (a) flow in a circular pipe (Eq. (4.17)) and (b) flow in a channel (Eq. (4.30)).	134
Figure 4.3	Variation of effective axial diffusivity with yield stress r_p and x_p for different values of chemical reaction rate parameter \bar{R} at Péclet number $Pe = 4$, power-law index $n = 0.95$ and $n = 1.05$ for some non-Newtonian fluids for (a) flow in a circular pipe (Eq. (4.17)) and (b) flow in a channel (Eq. (4.30)).	135
Figure 4.4	Variation of relative axial diffusivity with chemical reaction rate parameter \bar{R} for different values of yield stress r_p and x_p at power-law index $n = 0.95$ for (a) flow in a circular pipe (Eq. (4.18)) and (b) flow in a channel (Eq. (4.31)).	139
Figure 4.5	Variation of relative axial diffusivity of the solute with yield stress r_p and x_p at chemical reaction rate parameter $\bar{R} = 10$ for some non-Newtonian fluid models for flow in a circular pipe (Eq. (4.18)) and a channel (Eq. (4.31)).	140
Figure 5.1	Variation of steady dispersion function with radius r and width x for different values of chemical reaction rate parameter α at power-law index $n = 0.95$ and yield stress $r_p = x_p = 0.1$ for H-B fluid and Casson fluid for (a) flow in a circular pipe and (b) flow in a channel.	176
Figure 5.2	Variation of steady dispersion function with radius r and width x for different values of yield stress r_p and x_p at chemical reaction rate parameter $\alpha = 0.1$ and power-law index $n = 0.95$ for H-B fluid for (a) flow in a circular pipe and (b) flow in a channel.	177
Figure 5.3	Variation of steady dispersion function with radius r and width x for different fluid models at yield stress $r_p = x_p = 0.1$ and chemical reaction rate parameter $\alpha = 0.1$ for (a) flow in a circular pipe and (b) flow in a channel.	178

Figure 5.4	Variation of unsteady dispersion function with radius r and width x for different values of chemical reaction rate parameter α at yield stress $r_p = x_p = 0.1$, $n = 0.95$ and time $t = 0.1$ for H-B fluid for (a) flow in a circular pipe (Eq. (5.66)) and (b) flow in a channel (Eq. (5.131)).	182
Figure 5.5	Variation of unsteady dispersion function with radius r for different values of time t in a circular pipe (Eq. (5.66)) at chemical reaction rate parameter $\alpha = 0.1$, power-law index $n = 0.95$ and yield stress (a) $r_p = 0$, (b) $r_p = 0.05$, (c) $r_p = 0.1$ and (d) $r_p = 0.2$.	183
Figure 5.6	Variation of unsteady dispersion function with width x for different values of time t in a channel (Eq. (5.131)) at chemical reaction rate parameter $\alpha = 0.1$, power-law index $n = 0.95$ and yield stress (a) $x_p = 0$, (b) $x_p = 0.05$, (c) $x_p = 0.1$ and (d) $x_p = 0.2$.	184
Figure 5.7	Variation of unsteady dispersion function with radius r and width x for different fluid models at yield stress $r_p = x_p = 0.1$, time $t = 0.1$ and chemical reaction rate parameter $\alpha = 0.1$ for (a) flow in a circular pipe (Eq. (5.66)) and (b) flow in a channel (Eq. (5.131)).	185
Figure 5.8	Variation of dispersion function with radius r for different values of time t in a circular pipe (Eq. (5.51)) at chemical reaction rate parameter $\alpha = 0.1$, power-law index $n = 0.95$ and yield stress (a) $r_p = 0$, (b) $r_p = 0.05$, (c) $r_p = 0.1$ and (d) $r_p = 0.2$.	187
Figure 5.9	Variation of dispersion function with width x for different values of time t in a channel (Eq. (5.119)) at chemical reaction rate parameter $\alpha = 0.1$, power-law index $n = 0.95$ and yield stress (a) $x_p = 0$, (b) $x_p = 0.05$, (c) $x_p = 0.1$ and (d) $x_p = 0.2$.	188
Figure 5.10	Variation of longitudinal diffusion coefficient with time t for different values of yield stress r_p and x_p at chemical reaction rate parameter $\alpha = 0.1$ and power-law index $n = 0.95$ for (a) flow in a circular pipe (Eq. (5.70)) and (b) flow in a channel (Eq. (5.135)).	191
Figure 5.11	Variation of longitudinal diffusion coefficient with time t for different values of chemical reaction rate parameter α and power-law index n at yield stress $r_p = x_p = 0.1$ for H-B fluid for (a) flow in a circular pipe (Eq. (5.70)) and (b) flow in a channel (Eq. (5.135)).	192

Figure 5.12	Variation of relative effective axial diffusivity (Eq. (5.71)) with time t for different values of yield stress at chemical reaction rate parameter $\alpha = 0.1$ and power-law index $n = 0.95$ for H-B fluid for (a) flow in a circular pipe and (b) flow in a channel.	194
Figure 5.13	Variation of relative effective axial diffusivity (Eq. (5.71)) with time t for different values of yield stress at chemical reaction rate parameter $\alpha = 0.1$ and power-law index $n = 1.05$ for H-B fluid for (a) flow in a circular pipe and (b) flow in a channel.	195
Figure 5.14	Variation of mean concentration of the solute (Eq. (5.85)) with time t for different values of chemical reaction rate parameter α , yield stress r_p/x_p and power-law index n at $z_s = 0.5$, $z = 0.5$ and $Pe = 1000$ for (a) flow in a circular pipe and (b) flow in a channel.	201
Figure 6.1	The geometries of fluid flow with irreversible absorption into wall tissues and reversible phase exchange between fluid and wall for (a) flow in a circular pipe and (b) flow in a channel.	206
Figure 6.2	Variation of negative asymptotic exchange coefficient (Eq. (6.67)) with wall absorption parameter β for different values of Damköhler number Da and partition coefficient σ for H-B fluid for (a) flow in a circular pipe and (b) flow in a channel.	239
Figure 6.3	Comparison of negative asymptotic convection coefficient with wall absorption parameter β for different values of Damköhler number Da and partition coefficient σ at yield stress $r_p = 0.1$ and for H-B fluid ($n = 0.95$), Casson fluid and Newtonian fluid ($n = 1, r_p = 0$) for flow in a circular pipe (Eq. (6.76)).	241
Figure 6.4	Variation of negative asymptotic convection coefficient with wall absorption parameter β for different values of Damköhler number Da and partition coefficient σ in a circular pipe (Eq. (6.76)) at $n = 0.95$ and (a) $r_p = 0$, (b) $r_p = 0.1$, (c) $r_p = 0.15$ and (d) $r_p = 0.2$.	243
Figure 6.5	Variation of negative asymptotic convection coefficient with wall absorption parameter β for different values of Damköhler number Da and partition coefficient σ in a channel (Eq. (6.153)) at $n = 0.95$ and (a) $x_p = 0$, (b) $x_p = 0.1$, (c) $x_p = 0.15$ and (d) $x_p = 0.2$.	244

Figure 6.6	Variation of longitudinal diffusion coefficient with wall absorption parameter β for different values of Damköhler number Da and partition coefficient σ in a circular pipe (Eq. (6.88)) at $n = 0.95$ and yield stress (a) $r_p = 0$, (b) $r_p = 0.1$, (c) $r_p = 0.15$ and (d) $r_p = 0.2$.	250
Figure 6.7	Variation of longitudinal diffusion coefficient of with wall absorption parameter β for different values of Damköhler number Da and partition coefficient σ in a channel (Eq. (6.162)) at $n = 0.95$ and yield stress (a) $x_p = 0$, (b) $x_p = 0.1$, (c) $x_p = 0.15$ and (d) $x_p = 0.2$.	251
Figure 6.8	Variation of mean concentration of the solute (Eq. (6.103)) with time t at yield stress $r_p = x_p = 0.1$, $z = 0.5$, $Da = 0.1$, $\sigma = 0.5$, $\beta = 0.01$ and $n = 0.95$ for H-B fluid for flow in a circular pipe and a channel.	254
Figure 6.9	Variation of mean concentration of the solute (Eq. (6.103)) with time t for different values of Damköhler number Da at yield stress $r_p = x_p = 0.1$, $z = 0.5$, $\sigma = 0.5$ and $\beta = 0.01$ for H-B fluid ($n = 0.95$) and Casson fluid for (a) flow in a circular pipe and (b) flow in a channel.	255

LIST OF ABBREVIATIONS

erf	Error function
FCT	Flux-Corrected Transport
GDM	Generalized Dispersion Model
H-B	Herschel-Bulkley
IFT	Inverse Fourier Transform
K-L	Kuang-Luo

LIST OF SYMBOLS

\bar{a}	Radius of the pipe flow
$a_1 - a_4$	Constant of velocity integration
A	Product of mean velocity in a circular pipe
A_m	Expansion coefficient for $m = 0, 1, 2, \dots$
\bar{A}_c	Cross-sectional area of conduits
$b_1 - b_4$	Constant of characteristic velocity integration
B	Product of relative velocity in the plug flow region in a circular pipe
B_m	Expansion coefficient for $m = 0, 1, 2, \dots$
c_1, c_2	Boundary condition of mean concentration in Fourier Transform
\bar{C}	Local concentration of the solute
C	Non-dimensional local concentration of the solute
\bar{C}_0	Reference concentration
\bar{C}_1, \bar{C}_2	Concentration of the solute in the plug and outer flow regions, respectively
C_m	Mean concentration of the solute
\tilde{C}_m	Mean concentration of the solute in Fourier transform
\bar{C}_p	Concentration of the solute at the plug flow region
\bar{C}_s	Concentration of the solute at immobile phase
C_s	Non-dimensional concentration of the solute at immobile phase
\bar{d}	Radius/semi-width of the cross section solute concentric with circular pipe/channel

d	Non-dimensional radius/semi-width of the cross section solute concentric with circular pipe/channel
D	Diameter of the conduits
Da	Damköhler number for reversible reaction
Dn	Dean number
\bar{D}_{eff}	Effective axial diffusivity
\bar{D}_m	Molecular diffusivity
E	Measure of the total reduction in dispersion without chemical reaction in a circular pipe
E/A^2	Effect of the distorted velocity profile for steady dispersion without chemical reaction in a circular pipe
$f(\bar{\tau})$	Flow curve
f_i	Dispersion function for $i = 0, 1, 2, \dots$
f_{1s}	Dispersion function of steady state
f_{1s_-}	Dispersion function of steady state in the plug flow region
f_{1s_+}	Dispersion function of steady state in the outer flow region
f_{1u}	Dispersion function of unsteady state
F	Product of mean velocity in a channel
\bar{g}	Gravitational acceleration
$\bar{g}_{\bar{r}}, \bar{g}_{\bar{x}}, \bar{g}_{\bar{y}}, \bar{g}_{\bar{z}}, \bar{g}_{\bar{\psi}}$	Gravitational acceleration in $\bar{r}, \bar{x}, \bar{y}, \bar{z}$ and $\bar{\psi}$ directions, respectively
G	Product of relative velocity in the plug flow region in a channel
\bar{h}	Semi-width of the channel
H	Measure of the total reduction in dispersion with chemical reaction in a channel

H/F^2	Effect of the distorted velocity profile for steady dispersion with chemical reaction in a channel
I_0	Modified Bessel function of the first kind of zeroth order
I_1, I_2	Integration of the flow rate without a chemical reaction in plug and outer flow regions for a circular pipe, respectively
I_3, I_4	Integration of the flow rate without a chemical reaction in plug and outer flow regions for a channel, respectively
I_5, I_6	Integration of the flow rate with a chemical reaction in plug and outer flow regions for a circular pipe, respectively
I_7, I_8	Integration of the flow rate with a chemical reaction in plug and outer flow regions for a channel, respectively
I_9, I_{10}	Integration of A_m with a chemical reaction in plug and outer flow regions for a circular pipe, respectively
I_{11}, I_{12}	Integration of A_m with a chemical reaction in plug and outer flow regions for a channel, respectively
J_0, J_1	Bessel functions of first kind of zeroth and first order, respectively
\bar{k}_1, \bar{k}_2	Irreversible and reversible reaction rate constants of the dispersion at the wall, respectively
K_i	Transport coefficient for $i = 0, 1, 2, \dots$
K_0, K_1, K_2	Exchange, longitudinal convection and dispersion (diffusion) coefficients, respectively
\bar{l}	Second order differential equation
l	Non-dimensional second order differential equation
\bar{L}	Length of the conduit
L	Dimension of length
\bar{L}_e	Conduit length in entrance region
M	Dimension of mass
\bar{M}_s	Mass of solute

n	Power-law index
N	Measure of the total reduction in dispersion without chemical reaction in a channel
N/F^2	Effect of the distorted velocity profile for steady dispersion without chemical reaction in a channel
\bar{p}	Fluid pressure
\bar{p}_1, \bar{p}_2	Fluid pressures at the entry and end of conduit in fully-developed, respectively
\bar{p}_e	Pressure in entrance region
Pe	Péclet number
\bar{q}	Flux of solute
Q_{conv}	Flux of convection
Q_{diff}	Flux of diffusion
$(Q_{diff})_{\bar{r}}, (Q_{diff})_{\bar{x}}, (Q_{diff})_{\bar{y}}, (Q_{diff})_{\bar{z}}$	Flux of diffusion in \bar{r} , \bar{x} , \bar{y} and \bar{z} directions, respectively
\bar{r}	Radial coordinate for pipe flow
r	Non-dimensional radial coordinate for pipe flow
\bar{r}_p	Radius of the plug flow region in a pipe
r_p	Non-dimensional radius of the plug flow region
\bar{R}	Chemical reaction rate parameter
Re	Reynolds number
\bar{t}	Time
t	Non-dimensional time
T	Dimension of time
T_1, T_2	Function of integration I_2

\bar{u}	Axial velocity of the fluid flow
$\bar{u}_{\bar{r}}$	Velocity in the \bar{r} direction
$\bar{u}_{\bar{x}}$	Velocity in the \bar{x} direction
$\bar{u}_{\bar{y}}$	Velocity in the \bar{y} direction
$\bar{u}_{\bar{z}}$	Velocity in the \bar{z} direction
$\bar{u}_{\bar{\psi}}$	Velocity in the $\bar{\psi}$ direction
\bar{u}_{+}	Axial velocity in the outer flow region
\bar{u}_{-}	Axial velocity in the plug flow region
\bar{u}_m	Mean velocity of the fluid
\bar{u}_0	Characteristic velocity
\hat{u}_{-}	Relative velocity in the plug flow region
\hat{u}_{+}	Relative velocity in the outer flow region
u_{+}	Non-dimensional axial velocity in the outer flow region
u_{-}	Non-dimensional axial velocity in the plug flow region
u_m	Non-dimensional mean velocity
\mathbf{U}	Vector of fluid velocities
\bar{V}	Volume of solution
W_1, W_2	Function of integration I_4
\bar{x}	Transverse coordinate for channel
x	Non-dimensional radius of transverse coordinate for a channel
\bar{x}_p	Semi-width of the plug flow region in a channel
x_p	Non-dimensional semi-width of the plug flow region

\bar{X}_1, \bar{X}_2	Separable function of \bar{z} and \bar{x} , respectively in a channel flow
X_1, X_2	Non-dimensional separable function of z and x , respectively in a channel flow
\bar{y}	Direction in Cartesian coordinate
Y	Measure of the total reduction in dispersion with chemical reaction in a circular pipe
Y/A^2	Effect of the distorted velocity profile for steady dispersion with chemical reaction in a circular pipe
\bar{Y}_1, \bar{Y}_2	Separable functions of \bar{z} and \bar{r} , respectively, in a circular pipe
Y_1, Y_2	Non-dimensional separable functions of z and r , respectively, in a circular pipe
\bar{z}	Axial coordinate for a circular pipe and a channel
z	Non-dimensional axial coordinate for a circular pipe and a channel
\bar{z}_s	Solute length
z_s	Non-dimensional solute length
\bar{z}_1	New axial coordinate for unsteady dispersion
z_1	Non-dimensional new axial coordinate for unsteady dispersion
\tilde{z}	New axial coordinate for steady dispersion
$\Delta \bar{t}$	Time interval
∇	Gradient operator
Greek symbols	
α	Non-dimensional chemical reaction rate parameter
β	Wall absorption parameter for irreversible reaction
$\bar{\delta}$	Dirac delta function

δ	Non-dimensional Dirac delta function
δ_{ij}	Kronecker delta
Δ	Delta
ϕ, ν	Angular frequency
$\bar{\gamma}$	Shear rate
$\bar{\eta}_B$	Viscosity of Bingham plastic fluid model
$\bar{\eta}_C$	Viscosity of Casson fluid model
$\bar{\eta}_H$	Viscosity of H-B fluid model
$\bar{\eta}_P$	Viscosity of power-law fluid model
λ_m	Root of the equation
$\bar{\mu}$	Viscosity of Newtonian fluid model
$\bar{\rho}$	Density of the fluid
$\bar{\sigma}$	Partition coefficient
σ	Non-dimensional partition coefficient
$\bar{\tau}$	Shear stress
τ	Non-dimensional shear stress
$\bar{\tau}_y$	Yield stress
τ_y	Non-dimensional yield stress
$\bar{\psi}$	Azimuthal angle
ψ	Non-dimensional azimuthal angle
ω	Integral of K_0 in Eq. (6.100)
ζ	Integral of K_1 in Eq. (6.101)
ξ	Integral of K_2 in Eq. (5.84) and (6.102)

**ANALISIS MATEMATIK BAGI MODEL BENDALIR
HERSCHEL-BULKLEY UNTUK PENYEBARAN BAHAN LARUT
DALAM ALIRAN DARAH MELALUI KONDUIT SEMPIT**

ABSTRAK

Penyebaran bahan larut memainkan peranan penting dalam pelbagai aplikasi kejuruteraan kimia, kejuruteraan bioperubatan dan sains alam sekitar. Kepentingan utama kajian ini adalah penyebaran bahan larut (ubat) dalam aliran darah (pelarut). Model matematik yang sesuai diperlukan bagi mengkaji penyebaran bahan larut dalam aliran darah. Dalam kajian ini, penyebaran bahan larut dalam aliran darah dianalisis secara matematik, dengan menyifatkan darah sebagai model bendalir Herschel-Bulkley (H-B) yang melalui conduit sempit iaitu paip bulat dan saluran antara dua plat rata yang selari. Penyebaran bahan larut yang mantap tanpa/dengan kehadiran tindak balas kimia antara bahan larut dan darah telah dipertimbangkan. Kemudiannya, kajian dikembangkan kepada penyebaran bahan larut tak mantap dengan tindak balas kimia. Akhir sekali, penyebaran bahan larut tak mantap dengan penyerapan bahan larut tak berbolak-balik ke tisu-tisu dinding dan pertukaran fasa yang berbolak-balik antara bendalir dan dinding dikaji dengan menggunakan model penyebaran teritlak. Sistem persamaan pembezaan tak linear yang terhasil diselesaikan secara analitik bagi memperoleh tegasan ricih, tegasan alas dan halaju normal darah. Ungkapan-ungkapan bagi kepekatan bahan larut, kemeresapan paksi efektif, kemeresapan paksi relatif, fungsi penyebaran, pekali-pekali pertukaran fasa, perolakan dan penyebaran diperoleh. Kepentingan kesan tegasan alah, indeks hukum kuasa, parameter kadar tindak balas kimia, parameter penyerapan dinding, nombor Péclet, nombor Damköhler dan pekali pembahagi fasa dibincangkan melalui graf-graf dan jadual-jadual yang bersesuaian. Didapati bahawa halaju normal darah dan

kemeresapan paksi efektif menurun apabila tegasan alah dan indeks hukum kuasa meningkat. Kelakuan berbeza ditunjukkan oleh purata kepekatan bahan larut. Keputusan menunjukkan tindak balas kimia, pekali pertukaran fasa dan pekali perolakan mengurangkan keberkesanan penyebaran bahan larut. Didapati bahawa halaju normal darah dan kemeresapan paksi efektif lebih tinggi apabila darah dimodelkan sebagai bendalir H-B berbanding bendalir Casson dan boleh dibandingkan dengan bendalir-bendalir tak Newtonan yang lain. Halaju normal darah, kemeresapan paksi efektif, pekali pertukaran fasa dan purata kepekatan lebih tinggi apabila darah mengalir melalui paip bulat berbanding dengan darah yang mengalir melalui saluran antara dua plat rata yang selari. Beberapa keputusan yang diperoleh dalam tesis ini menunjukkan hasil perbandingan yang baik dengan keputusan yang diterbitkan oleh kajian lepas.

MATHEMATICAL ANALYSIS OF HERSCHEL-BULKLEY FLUID MODEL FOR SOLUTE DISPERSION IN BLOOD FLOW THROUGH NARROW CONDUITS

ABSTRACT

The dispersion of solute play an important role in many chemical engineering, biomedical engineering and environmental sciences applications. The main interest of this study is the dispersion of solute (medicine) in blood (solvent) flow. An appropriate mathematical model is required to investigate the dispersion of solute in blood flow. In this study, the dispersion of solute in a blood flow is analyzed mathematically by treating the blood as a Herschel-Bulkley (H-B) fluid model through narrow conduits, namely, a circular pipe and a channel between two parallel flat plates. The steady dispersion of solute in blood flow without/with the presence of a chemical reaction between the solute and blood are considered. Then, the study is extended to investigate the unsteady dispersion of solute with chemical reaction. Finally, the unsteady dispersion of solute with irreversible absorption of solute to the wall tissues and reversible phase exchange between fluid and wall is studied using the generalized dispersion model. The resulting system of nonlinear differential equations is solved analytically to get the shear stress, yield stress and normalized velocity of the blood. The expressions for the concentration of solute, effective axial diffusivity, relative axial diffusivity, dispersion function, phase exchange, longitudinal convection and dispersion coefficients are obtained. The effects of yield stress, power-law index, chemical reaction rate parameter, wall absorption parameter, Péclet number, Damköhler number and phase partition coefficient are discussed through appropriate graphs and tables. It is seen that the normalized velocity of blood and the effective axial diffusivity decrease as the yield stress and power-law index

increase. The reversed behavior is shown by a mean concentration of solute. Results indicate that the chemical reaction, phase exchange and convection coefficients reduce the effectiveness of solute dispersion. It is noted that the normalized velocity of blood and effective axial diffusivity are higher when blood is treated as a H-B fluid rather than a Casson fluid and are comparable to other non-Newtonian fluids such as Bingham and power-law fluids. The normalized velocity of blood, effective axial diffusivity, phase exchange coefficient and mean concentration are higher when blood flows through a circular pipe than when it flows in a channel between two parallel flat plates. Some of the results obtained in this thesis are found to be in a good agreement with other published results from the literature.

CHAPTER 1

INTRODUCTION

1.1 Background of Study

The dispersion of solute in a solvent flowing through a pipe or channel is broadly investigated by many researchers because it has numerous applications in various fields of science and engineering. Some of the potential fields are chemical engineering (Marrero & Mason, 1972; Kuehn & Goldstein, 1976; Carli & Byers, 1990), biomedical engineering (Gentile et al., 2008; Vikhansky & Wang, 2011), physiological fluid dynamics (Agrawal & Jayaraman, 1994) and environmental sciences (Mercer & Roberts, 1990, 1994). Some specific applications of this research area are the mixing and transport of drugs or toxins in physiological systems, the transport of pollutants in the environment, the dispersion of gaseous tracer in chemical engineering and also the chromatographic separations in chemical engineering.

One of the main applications that attracted the interest among the researchers is the dispersion of solute (medicine) in blood flow through conduits in the cardiovascular system (Ananthakrishnan et al., 1965; Ghoshal et al., 1971; Booras & Krantz, 1976; Chandra & Agarwal, 1983; Patel & Sirs, 1983; Sharp, 1993; Bandyopadhyay & Mazumder, 1999; Azer, 2005; Gentile et al., 2007, 2008; Gentile & Decuzzi, 2010). There are many cardiovascular diseases that affect the blood flow such as emphysema (the alveoli of the lungs lose their elasticity and may finally tear), anemia (loss of red blood cell and hemoglobin in blood) and pulmonary hypertension (Scott & Fong, 2009). Therefore, patients with cardiovascular diseases

need to take medicine to treat the diseases. Absorption of medicine into the body depends on several factors such as the route of administration uptake, the dosage form, the amount of medicine, the pH of blood and the solubility of medicine (Ritschel & Kearns, 2009). For example, taking capsules or liquids orally is recommended when the medicine must be given slowly but frequently. Enzymes in the stomach may break down certain slight medicine and it will reduce the concentration of the medicine. The medicine becomes less effective and therefore, the patients must take the medicine frequently. All these factors are involved in determining whether the medicine administered will produce a therapeutic effect, yield only subtherapeutic effect or even show toxic effects (Ritschel & Kearns, 2009). In emergencies such as heart attack or stroke, the patients must receive medicine immediately. Thus, the medicine needs to be given directly into the bloodstream via intravenous medication. Intravenous is a term that means “into the vein”. Intravenous medication is given by injection into the vein. The intravenous medication is necessary for certain diseases because it has many advantages such as an effective dose can be determined and it has faster absorption than the oral administration. Since many intravenous medications are therapeutic at low concentration, but toxic at high concentration, the study on the shear-augmented dispersion of solute at low concentration in blood flow plays an important role in the treatment of many cardiovascular diseases (Sharp, 1993).

The main interest of this study is the dispersion of solute in blood flow, especially in narrow arteries. The study may help in understanding several physiological processes that includes injecting an amount of medicine into the bloodstream and to compute the concentration of medicine at some points. To study

the solute dispersion in blood flow, the field of fluid mechanics is required to analyze the changes of the blood properties when the solute is injected into the bloodstream. The development of the mathematical models using the properties of fluid mechanics could play an essential role in better understanding the complex phenomena related to the dynamics of blood flow. To investigate the dispersion of medicine in the bloodstream, mathematical models of blood are required. These mathematical models are currently being used for diagnosis and development of arterial diseases, surgical planning and therapy, and training system for new treatment procedure (Quarteroni & Formaggia, 2004). In this study, the knowledge of fluid mechanics has been applied to understand the blood properties in the cardiovascular system, to measure the velocity profile, the concentration of solute, the rate of dispersion process, the dispersion function and the transport coefficients. The presented results of this study may help physiologists in recommending appropriate amount of medicine to patients depending on the situation. In addition, the presented results are also very useful to pharmaceutical researchers to design more medicines that are effective.

In previous studies, many researchers treated the blood as Newtonian fluid and certain non-Newtonian fluids such as Casson, power-law and Bingham fluids when solving the solute dispersion. However, one of the most important mathematical models of blood known as Herschel-Bulkley (H-B) fluid model does not received attention of many researchers. Therefore, H-B fluid model will be used in this study to improve the description of the results as well as to get a realistic illustration of the real flow field. In addition, the previous researchers only investigated certain cases of the solute dispersion in blood flow by ignoring the chemical reactions that occurs

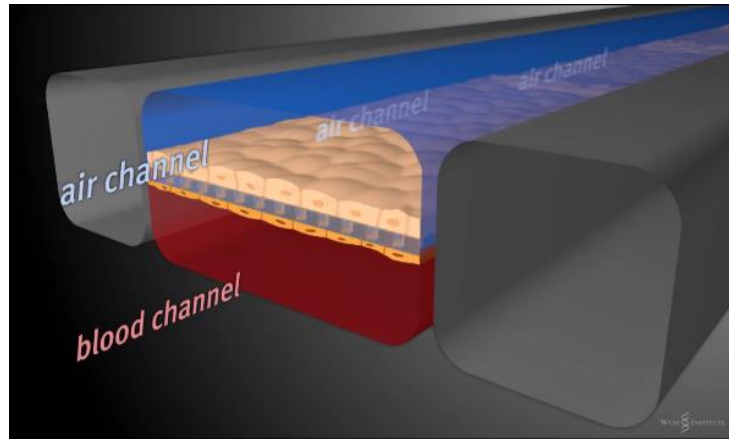


Figure 1.1: The Wyss Institute’s human breathing lung-on-a-chip. It is a microdevice the size of memory stick used for testing drug and toxin (Larkin, 2015).

between the solute and blood or arterial walls. Thus, the effects of the chemical reaction between the solute and blood, and the wall reactions to the blood flow will be considered in this study.

Hence, in the present study, the H-B fluid model has been used in four problems, namely, the steady dispersion of solute, steady dispersion of solute with chemical reaction, unsteady dispersion of solute with chemical reaction, and unsteady dispersion of solute with the effect of the solute absorption to the wall tissue and phase exchange between the blood and the wall. Since some clinical devices such as blood oxygenator (Dash et al., 2000) and lung-on-a-chip (Larkin, 2015) (shown in Figure 1.1) require the blood to flow through a channel between two parallel flat plates or membranes rather than in a circular pipe, we also investigate a solute dispersion through a channel between two parallel flat plates.

In order to investigate the dispersion of solute in blood flow, it is important to know four contexts of the study, namely the basics of the cardiovascular system, the

fluid models, the concepts of fluid mechanics and convective-diffusion equation. These four contexts will be discussed in the next sections.

1.2 Cardiovascular System

Figure 1.2 shows a diagram representation of the cardiovascular system (The human circulatory system, n.d.). The cardiovascular system or also known as circulatory system consists of blood vessels, heart and blood. The function of the cardiovascular system is to transport the blood throughout the body. The blood as a medium will transport the oxygen, nutrients and hormones to all parts of the body tissues, and the carbon dioxide and other waste products to be removed from the body. Besides, the function of the cardiovascular system is to protect the body against infections and diseases. The cardiovascular system is also important to regulate body pH and temperature (Mai, 2010) and to help maintain the fluid balance within the body (The cardiovascular system – more than a blood pump, n.d.).

The cardiovascular system can be divided into two types of circulatory paths which are the pulmonary circulation and the systemic circulation. The pulmonary circulation is a short loop which brings the deoxygenated blood from the heart to the lungs and back again with the oxygenated blood from the lungs to the heart. Meanwhile, the systemic circulation is a system that transmits the oxygenated blood from the heart to all parts of our body (organs and body tissues) and returns deoxygenated blood back to the heart (Boundless, 2015a).

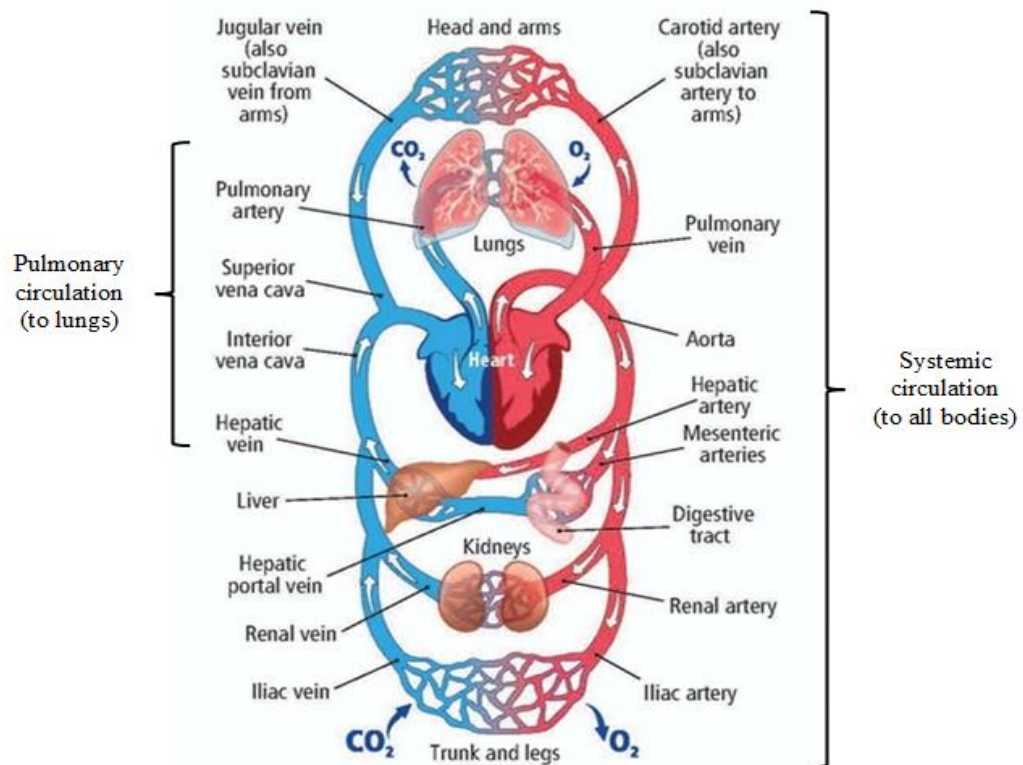


Figure 1.2: A diagram representation of the human cardiovascular system (The human circulatory system, n.d.).

1.2.1 The blood vessels

The blood vessels are the delivery paths (Elad & Einav, 2004). They carry the oxygenated blood from the lungs to all parts of the body and bring the deoxygenated blood again to the lungs. Blood is pumped through the blood vessels by heart. There are three major types of blood vessels named artery, vein and capillary and two sub-types known as arteriole and venule. Structures of the artery, vein, capillary, venule and arteriole are shown in Figure 1.3 (Arteries and veins, n.d.).

The arteries are the blood vessels with the largest diameter that carry the oxygenated blood away from the heart to all parts of the body. The largest artery is the aorta. Each artery is a muscular tube (consists of muscle) lined with smooth tissues. The arteries consist of three layers, namely the intima (the inner layer lined

with a smooth tissue called the endothelium), the media (the middle layer consists of a smooth muscle) and the adventitia (the outer layer consists of the connective tissues with elastic and collagen fibers). The media forces the blood along and helps the arteries handle the high pressures from the heart. The thick wall of artery contains a strong outer layer to support the pressure during blood circulation. The function of the connective tissue is to attach the artery to the adjacent tissues (Arteries and veins, n.d.).

On the other hand, veins are the blood vessels that carry the deoxygenated blood from various parts of the body towards the heart. The structure of a vein is similar to that of the structure of an artery which is also consists of three layers known as the intima, media and adventitia. However, the wall of a vein is thinner, less elastic and its lumens have a greater diameter than the artery because the blood pressure in vein is relatively lower than artery. The veins also have the valves in the lumen to prevent the back flow of the blood (Arteries and veins, n.d.).

Capillaries are the blood vessels with the smallest diameter and consist of a single wall layer known as endothelium. This one-cell-thick wall carries the blood from arteriole to venule. Venules are small blood vessels that connect the capillaries to veins, which carry deoxygenated blood back to the atria. Arterioles are small blood vessels that connect the capillaries to the arteries, which carry the blood to all parts of the body. Figure 1.4 shows the differences between an artery, a vein and a capillary (The human circulatory system, n.d.).

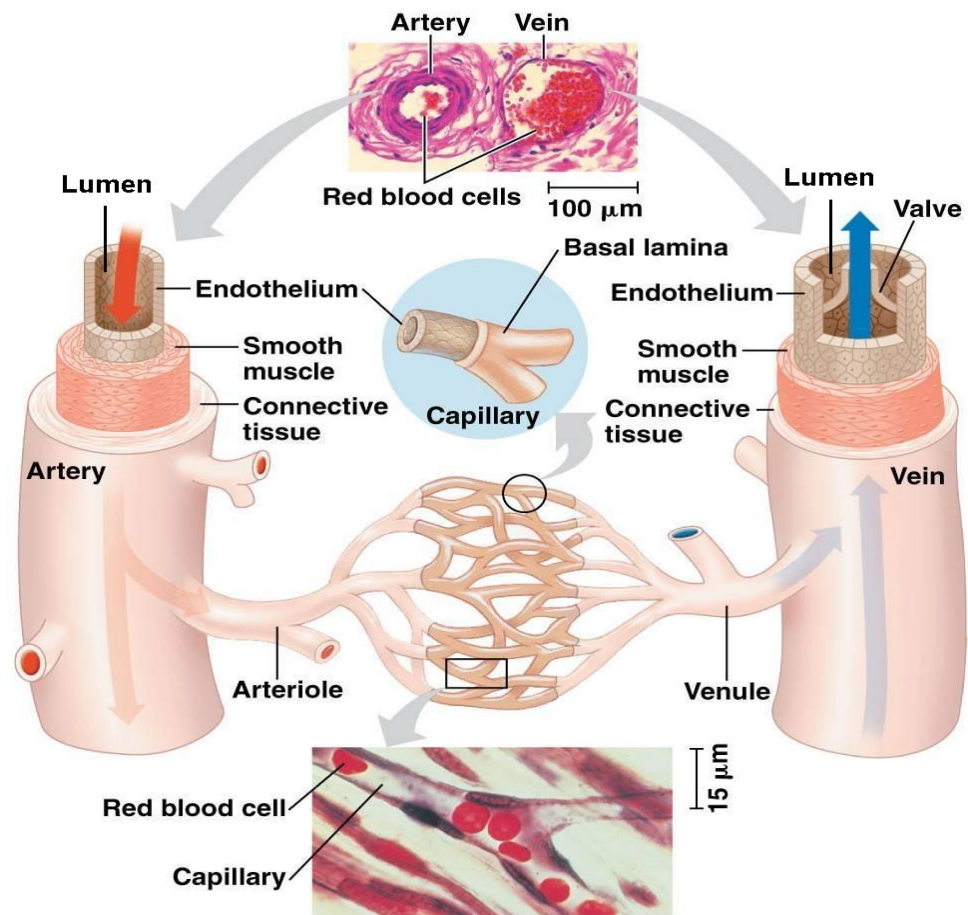


Figure 1.3: Structures of the artery, vein, capillary, venule and arteriole (Arteries and veins, n.d.).

Artery	Thick, elastic wall Endothelium Small lumen Smooth muscle
Vein	Thin wall Endothelium Large lumen Valve
Capillary	Very thin wall Endothelium Tiny lumen

Figure 1.4: The differences between an artery, a vein and a capillary (The human circulatory system, n.d.).

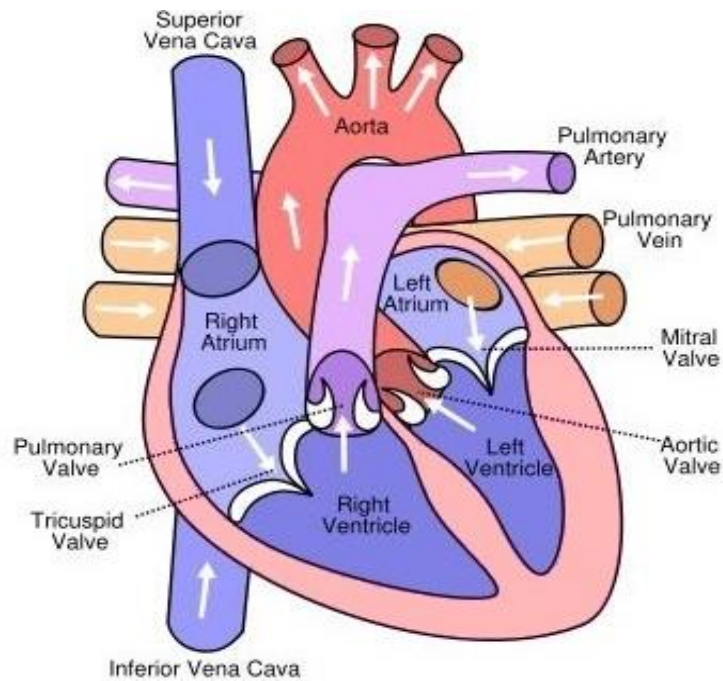


Figure 1.5: The structure of the heart (Boundless, 2015b).

1.2.2 The heart

The heart is a muscular organ that is located on the left side of the midline of the thoracic cavity. It is made out of cardiac muscle and a thin membrane surrounds it with two layers called pericardium. The heart acts as a pump that yields the pressure gradients. The pressure gradients are required to deliver the blood to all parts of the body tissues. The structure of the heart is shown in Figure 1.5 (Boundless, 2015b). The heart is divided into four chambers; the upper two chambers (left and right atria) and the lower two chambers (left and right ventricles). The atria and ventricles are separated by valves. The right valve is called the tricuspid, whereas the left valve is called the bicuspid (mitral). These valves control the filling of the heart ventricles (Boundless, 2015b).

The vena cava brings the deoxygenated blood into the right atrium. Then, the blood flows into the right ventricle. After the right ventricle is full with blood, the

blood is pumped out into the right and left pulmonary arteries. Then, the blood moves to the lungs for oxygenation. The oxygenated blood from the pulmonary circulation enters the left atrium from the pulmonary veins and then the blood is pumped into the left ventricle. The blood flows from the left ventricle into the aorta to all the body parts (systemic circulation) (Boundless, 2015b).

1.2.3 The blood

1.2.3(a) The constituents of blood

Blood is the suspension of mainly three types of corpuscles (particles) in continuous medium called plasma. The plasma consists of approximately 91% water by weight, 7% plasma protein, and 2% inorganic and organic substances. The particles in plasma consist of approximately 96% of erythrocytes or red blood cells, 3% of leukocytes or white blood cells and 1% of platelets. Erythrocytes contain hemoglobin to carry the oxygen around the body. The structure of erythrocytes is very simple which the size is approximately 8 μm in diameter (Identification of red & white blood cells, n.d., para. 2). Leukocytes are the largest particle compared to other cells, which are approximately 6-20 μm in diameter. The function of leukocytes is to defend the body against infections and injuries (Scott & Fong, 2009). They attack and produce the antibodies to destroy the bacteria. They also play a crucial role in blood transport around the body. In addition, platelets are the smallest particle compared to the leukocytes and erythrocytes. They are approximately 2-4 μm in diameter. Although small, they are extremely important in the process of blood clotting both in the healing of wounds and formation of thrombi (a fibrinous clot formed by an insoluble protein known as fibrinogen) (Identification of red & white blood cells, n.d., para. 9).

1.2.3(b) Blood rheology

To describe the blood, we have to understand the blood rheology. Rheology is a branch of physics that studies the deformation and flow of object which the fluid exhibits as non-Hookean (viscoelastic) and non-Newtonian behavior (Bird et al., 1960; Merrill, 1969).

Blood shows the anomalous behaviors when it flows through the arteries of different diameters (Sankar & Lee, 2008). Two types of anomaly are due to low and high shear effects. The blood shows Newtonian fluid's character when it flows in larger arteries (diameter > 3 mm) at a high shear rate (strain rate) or velocity gradient. However, when it flows in narrow arteries (diameter < 3 mm) at a low shear rate, it exhibits noticeable non-Newtonian fluid behavior (Dash et al., 1996; Tu & Deville, 1996; Lee & Smith, 2012; Sankar & Yatim, 2012). The velocity of blood can be significantly different when it flows in narrow arteries because of the accumulation of the red blood cells at the central region of the arteries (known as the plug core region or plug flow region).

The non-Newtonian fluid may exhibit a yield stress. The yield stress is a starting point for a new state and it exists when the blood flows from a normal flow to abnormal flow. The yield stress arises from the accumulation of red blood cells in the flow due to the presence of fibrinogen and globulin at a low shear rate to form three-dimensional micro-structures called a rouleaux (Sochi, 2014). The rouleaux will increase in particle size which causes distortion of the blood flow and higher frictional resistance between them, thereby increase in blood viscosity (Mandal, 2016). Merrill (1969) and Lou and Yang (1993) discovered that the yield stress is

positively related to the concentration of fibrinogen protein and the hematocrit level (volume percentage of red blood cells in whole blood). Cokelet et al. (1963) presented that as the shear rate increases, the rouleaux decreases until the red blood cells exist only as individuals and it behaves as a Newtonian fluid.

Since the effect of non-Newtonian fluid on the blood rheology is highly dependent on the geometry (either pipe or channel) and the size of the vessels, the different non-Newtonian rheological behaviors and hence, the different flow modeling approaches should be applied to different parts of the cardiovascular system (Sochi, 2014). Some non-Newtonian fluid models have been used to describe the blood rheology including Casson fluid (Morris et al., 1987; Fisher & Rossmann, 2009), Bingham fluid (Lou & Yang, 1993), Oldroyd-B (Perktold et al., 1999), Carreau-Yasuda fluid (Gijssen et al., 1999; Fisher & Rossmann, 2009), Ree-Eyring fluid (Marcinkowska-Gapińska et al., 2007), Cross fluid (Kim et al., 2008), Quemada fluid (Kim et al., 2008), Yeleswarapu fluid (Yilmaz & Gundogdu, 2008), power-law fluid (Fisher & Rossmann, 2009; Revellin et al., 2009), H-B fluid (Sankar & Ismail, 2009), Eyring-Powell fluid (Zueco & Bég, 2009), Kuang-Luo (K-L) fluid (Sriyab, 2014) and Walburn-Schneck fluid (Malek et al., 2015).

1.3 The Fluid Models

Much of the modeling in non-Newtonian fluids concentrates on finding a constitutive. The constitutive equation is the relationship which allows stress to be calculated as a function of the kinematic variables and ultimately as a function of the possibly time-dependent velocity field (Astarita & Marrucci, 1974). The fluid flows continuously and always deforms under different shear stress. Shear stress is the force per unit area created when a tangential force acts on a surface. Figure 1.6

summarizes the relationship between the shear stress and shear rate (velocity gradient) for Newtonian and certain non-Newtonian fluids such as dilatant power-law, pseudoplastic power-law, H-B and Casson fluid models, where $\bar{\tau}$ is the shear stress, $\bar{\tau}_y$ is the yield stress, $\bar{\gamma}$ is the shear rate and n is the power-law index. The slope of the shear stress and shear rate is known as a fluid viscosity. Note that the viscosity of Newtonian fluid is dependent on the pressure and temperature but independent of the shear rate, as presented by the linear relation between shear stress and shear rate (Bird et al., 1960; Papaioannou & Stefanadis, 2005). Meanwhile, for non-Newtonian fluids, the viscosity depends on the pressure, temperature and shear rate (Bird et al., 1960; Papaioannou & Stefanadis, 2005). In addition, this figure shows a critical value of the shear stress known as the yield stress $\bar{\tau}_y$. Casson, H-B and Bingham plastic fluids are the fluid models exhibit the yield stress $\bar{\tau}_y$. The aforesaid fluids act as elastic solids (no flow occurs) below a critically applied stress ($\bar{\tau} \leq \bar{\tau}_y$) before the fluids begin to flow (Bird et al., 1960; Callahan, 2011). Moreover, H-B and power-law fluids exhibit the power-law index n . The behavior when $n < 1$ is called shear thinning (fluid's viscosity decreases with increasing shear stress) and when $n > 1$ is called the shear thickening (fluid's viscosity increases with increasing shear stress). When $n = 1$, H-B fluid model will reduce to Bingham plastic fluid model and power-law model will reduce to Newtonian fluid model.

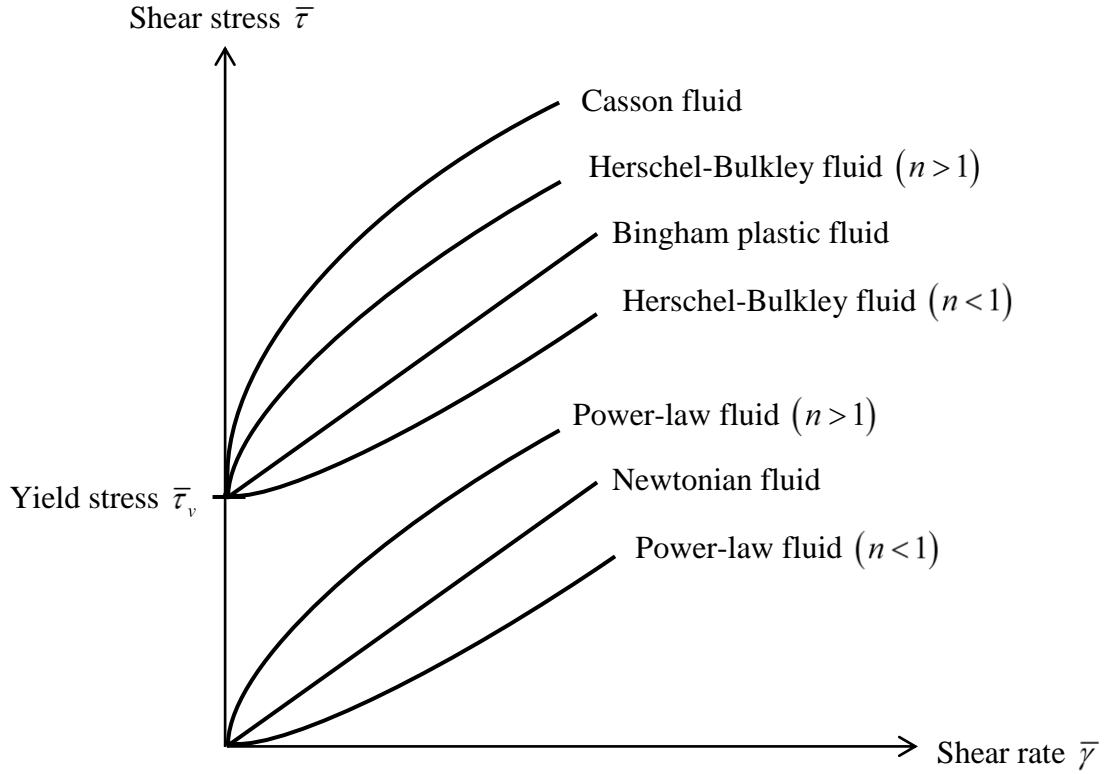


Figure 1.6: The relationship between the shear stress and shear rate for Newtonian and certain non-Newtonian fluids.

1.3.1 Newtonian fluid model

A Newtonian fluid model is a fluid for which the shear stress is linearly proportional to the shear rate (Cengel & Cimbala, 2006). The constitutive equation for this fluid is described by the Newton's law of viscosity, which is represented as (Papaioannou & Stefanadis, 2005)

$$\bar{\gamma} = \frac{\bar{\tau}}{\bar{\mu}}, \quad (1.1)$$

where $\bar{\tau}$ is the shear stress, $\bar{\gamma}$ is the shear rate and $\bar{\mu}$ is the dynamic viscosity with dimension $ML^{-1}T^{-1}$, where M is the dimension of mass, L is the dimension of length and T is the dimension of time.

1.3.2 Non-Newtonian fluid models

In Eq. (1.1), the relationship between the shear stress and the shear rate is assumed to be linear. However, not all shear stress and shear rate obey this relationship for certain cases. The non-Newtonian fluid models show the non-linear relationship between the shear rate and shear stress as stated in Sochi (2014) which do not obey Newton's law of viscosity. The general form of the constitutive equation for non-Newtonian fluid model is given by (Astarita & Marrucci, 1974)

$$\bar{\gamma} = f(\bar{\tau}), \quad (1.2)$$

where $f(\bar{\tau})$ denotes the flow curve illustrating the nature of a certain fluid. Some of the most generally used non-Newtonian fluid models are the power-law, Bingham, Casson and H-B fluid models (Scott, 2005). The viscosity of non-Newtonian fluid models depends strongly on the shear rate and known as shear viscosity (Owens & Philips, 2002). These fluid models will be discussed in the next section.

1.3.2(a) Power-law fluid model

The fluid model most generally used to describe the flow behavior of non-Newtonian fluid is a power-law fluid (Kucaba-Piętal, 2005). This fluid model is the generalization of Newtonian fluid model that introduces the power-law index n . The constitutive equation of power-law fluid model is (given by Sankar and Hemalatha (2006) when the yield stress of H-B is equal to zero)

$$\bar{\gamma} = \frac{\bar{\tau}^n}{\bar{\eta}_p}, \quad (1.3)$$

where $\bar{\eta}_p(\bar{\gamma}) = \bar{\mu} \bar{\gamma}^{n-1}$ is the viscosity of power-law fluid with dimension $(ML^{-1}T^{-2})^n T$. Note that the viscosity of this fluid $\bar{\eta}_p$ is a function of the shear rate (Bird et al., 1960). A derivation of viscosity of power-law fluid is given in

Appendix A. Eq. (1.3) can be reduced to the constitutive equations of Newtonian fluid when $n = 1$ (Bird et al., 1960).

1.3.2(b) Bingham plastic fluid model

A simple generalization of Newtonian fluid model that introduces the yield stress $\bar{\tau}_y$ is the Bingham plastic fluid model. The viscosity of Bingham plastic fluid exhibits a linear relationship between shear stress and shear rate as Newtonian fluid. The constitutive equation of Bingham plastic fluid model is (given by Sankar and Hemalatha (2006) when the power-law index of H-B is equal to one)

$$\bar{\gamma} = \begin{cases} \frac{1}{\bar{\eta}_B} (\bar{\tau} - \bar{\tau}_y) & \text{if } \bar{\tau} \geq \bar{\tau}_y, \\ 0 & \text{if } \bar{\tau} < \bar{\tau}_y, \end{cases} \quad (1.4)$$

where $\bar{\eta}_B(\bar{\gamma}) = \bar{\mu} - \bar{\tau}_y / \bar{\gamma}$ is the viscosity of Bingham fluid with dimension $ML^{-1}T^{-1}$ (Bird et al., 1960). A derivation of viscosity of Bingham fluid is given in Appendix A. Eq. (1.4) indicates that the normal shear flow (outer flow) occurs in the region when $\bar{\tau} \geq \bar{\tau}_y$, while the unshear flow (solid-like fluid or plug flow) occurs in the region when $\bar{\tau} < \bar{\tau}_y$. Eq. (1.4) can be reduced to the constitutive equations of Newtonian fluid when $\bar{\tau}_y = 0$ (Bird et al., 1960).

1.3.2(c) Casson fluid model

The Casson fluid model extends the power-law and Bingham fluid models. The Casson fluid consists of the yield stress similar to that of the Bingham fluid model. The constitutive equations of the Casson fluid model are (Sankar & Lee, 2011)

$$\bar{\gamma} = \begin{cases} \frac{1}{\bar{\eta}_c} \left(\sqrt{\bar{\tau}} - \sqrt{\bar{\tau}_y} \right)^2 & \text{if } \bar{\tau} \geq \bar{\tau}_y, \\ 0 & \text{if } \bar{\tau} < \bar{\tau}_y, \end{cases} \quad (1.5)$$

where $\bar{\eta}_c = \bar{\mu} - 2\sqrt{\bar{\tau}\bar{\tau}_y}/\bar{\gamma} + \bar{\tau}_y/\bar{\gamma}$ is the viscosity of Casson fluid with dimension $ML^{-1}T^{-1}$. A derivation of viscosity of Casson fluid is given in Appendix A. The Casson fluid model reduces to the Newtonian fluid model when $\bar{\tau}_y = 0$. Similar to Eq. (1.4), Eq. (1.5) can be reduced to the constitutive equations of Newtonian fluid when $\bar{\tau}_y = 0$ (Bird et al., 1960).

1.3.2(d) Herschel-Bulkley (H-B) fluid model

A simple generalization of Bingham plastic fluid model that introduces the power-law index n is the H-B fluid model. The constitutive equation of H-B fluid model is given as follows (Sankar & Hemalatha, 2006):

$$\bar{\gamma} = \begin{cases} \frac{1}{\bar{\eta}_H} \left(\bar{\tau} - \bar{\tau}_y \right)^n & \text{if } \bar{\tau} \geq \bar{\tau}_y, \\ \bar{\gamma} = 0 & \text{if } \bar{\tau} < \bar{\tau}_y, \end{cases} \quad (1.6)$$

where $\bar{\eta}_H(\bar{\gamma}) = \bar{\mu}^n \bar{\gamma}^{n-1} \left(1 - \bar{\tau}_y / \bar{\mu} \bar{\gamma} \right)^n$ is the viscosity of H-B fluid with dimension $(ML^{-1}T^{-2})^n T$. A derivation of viscosity of H-B fluid is given in Appendix A. Eq. (1.6) can be reduced to the constitutive equations of Newtonian fluid when $n=1$ and $\bar{\tau}_y = 0$, of power-law fluid when $n \neq 1$ and $\bar{\tau}_y = 0$ and of Bingham fluid when $n=1$ and $\bar{\tau}_y \neq 0$.

1.3.2(e) The advantages of Herschel-Bulkley (H-B) fluid

H-B and Casson fluid models are the non-Newtonian fluid models with yield stress. They are generally used in the studies of blood flow through narrow arteries (Siddiqui et al., 2009; Sankar & Lee, 2011). This section presents some reviews regarding the H-B and Casson fluid models. Scott Blair (1966) propounded that the H-B fluid model is easier to explain in most of blood flow cases. Scott Blair and Spanner (1974) and Tu and Deville (1996) reported that the blood behaves like Casson fluid only at moderate shear rate in smaller diameter arteries, whereas H-B fluid model can still be used at low shear rate of flow in very narrow arteries when the yield stress is high. Chaturani and Samy (1985) pointed out that when blood flows in arteries of diameter 0.095 mm, blood behaves like H-B fluid rather than power-law or Bingham fluids.

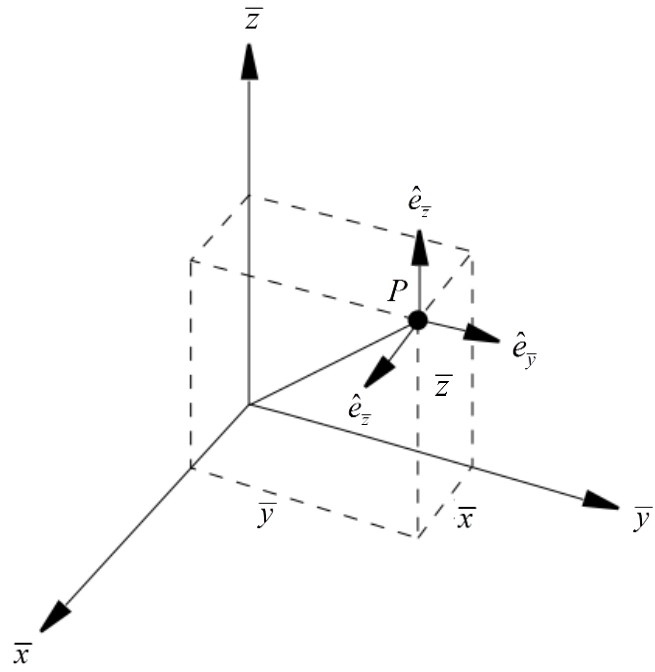
Iida (1978) reported that the velocity profile in the arterioles having diameter less than 0.1 mm can be generally explained by Casson and H-B fluid models when the yield stress is high. However, the velocity profile in the arterioles whose diameters are less than 0.065 mm does not conform to the Casson fluid model, but the blood could still be explained by H-B model. Iida (1978) reported that the residual variation which is the sum of the squares of the deviations of the observed values of stress from the estimated values of the stress is lower for H-B fluid model compared to Casson fluid model. In addition, Casson fluid's constitutive equation has only one parameter, namely the yield stress, whereas the H-B fluid's constitutive equation has one more parameter, namely the power-law index n . Thus, detailed information about blood flow properties would be retrieved using the H-B fluid

model rather than Casson fluid model (Sankar & Lee, 2009). H-B fluid model is also valid in arteries of diameter up to 1.3 mm.

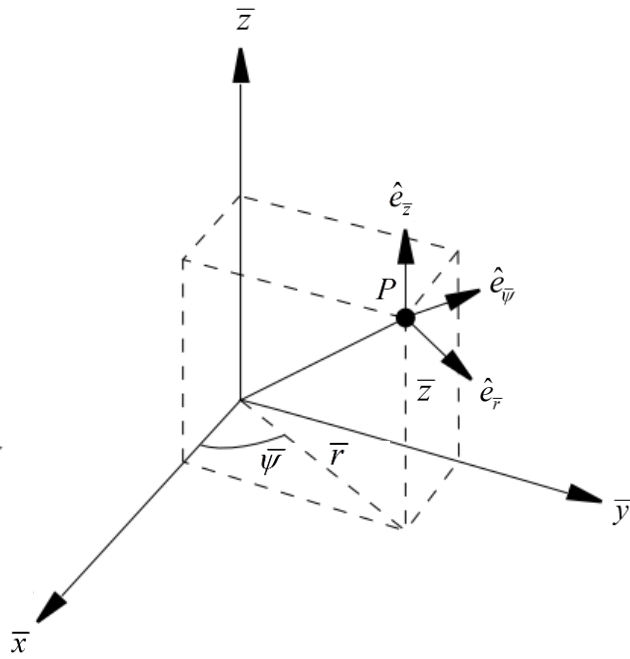
It is more appropriate to represent blood flow as H-B fluid model rather than Casson fluid model when it flows through smaller diameter arteries. Since H-B fluid model has several advantages over Casson fluid model through narrow arteries, it will be very useful to study the dispersion of solute in blood flow by treating the blood as H-B fluid model in this study through narrow arteries. The presented results of H-B fluid model can be reduced to Newtonian, power-law and Bingham fluid models. Thus, in this study, some of the results of H-B fluid are compared with Newtonian, power-law, Bingham and Casson fluid models from the previous literature. The study of H-B fluid in the solute dispersion can present better results. Comparing all the fluid models can be useful to verify which model is better when the solute disperses in blood flow through narrow arteries at low shear rate.

1.4 Basic Concepts of Fluid Mechanics

In order to study the solute dispersion in blood flow, it is important to know the basic concepts of fluid mechanics in the blood rheology. Hence, this section presents the Cartesian and cylindrical coordinate systems, type of flows, governing equations and dimensional analysis that are applicable to the study of blood rheology.



(a)



(b)

Figure 1.7: Coordinate of the point P for (a) Cartesian and (b) cylindrical coordinate systems (modified from Kay, 1964).

1.4.1 Cartesian and cylindrical coordinate systems

In this section, the two main systems of coordinates used in this study, namely Cartesian and cylindrical coordinate systems are presented. Figures 1.7(a) and (b) depict the coordinate of the point P for Cartesian and cylindrical coordinates, respectively. The coordinates in Cartesian coordinate system in Figure 1.7(a) are denoted by $(\bar{x}, \bar{y}, \bar{z})$ and the unit vectors along the \bar{x} , \bar{y} and \bar{z} directions are $\hat{e}_{\bar{x}}$, $\hat{e}_{\bar{y}}$ and $\hat{e}_{\bar{z}}$, respectively. Meanwhile, for the cylindrical coordinate system in Figure 1.7(b), the position of a point P is given by the radius of the cylinder \bar{r} with respect to the axis \bar{z} and the angle $\bar{\psi}$ to position the radius with respect to a reference direction and the height \bar{z} . Thus, the coordinates in cylindrical coordinate system are given by $(\bar{r}, \bar{\psi}, \bar{z})$ and the unit vectors along the \bar{r} , $\bar{\psi}$ and \bar{z} directions are $\hat{e}_{\bar{r}}$, $\hat{e}_{\bar{\psi}}$ and $\hat{e}_{\bar{z}}$, respectively. Note that, in this coordinate system, the unit vectors $\hat{e}_{\bar{r}}$ and $\hat{e}_{\bar{\psi}}$ change with the point in space. The Cartesian and cylindrical coordinate systems are related by (Kay, 1964)

$$\bar{x} = \bar{r} \cos \bar{\psi}, \quad (1.7)$$

$$\bar{y} = \bar{r} \sin \bar{\psi}, \quad (1.8)$$

$$\bar{z} = \bar{z}, \quad (1.9)$$

whereas the inverse transformations are

$$\bar{r} = \sqrt{\bar{x}^2 + \bar{y}^2}, \quad (1.10)$$

$$\bar{\psi} = \tan^{-1} \frac{\bar{y}}{\bar{x}}, \quad (1.11)$$

and \bar{z} as in Eq. (1.9).

1.4.2 Types of flow

1.4.2(a) Steady and unsteady flows

Steady flow occurs when the conditions and properties associated with the flow field do not change with time at various points of the flow field, where the flow field represents the characteristics of the fluid such as velocity, density, pressure and so on. The example of the steady flow is water being pumped through a fixed system at a constant rate. However, the flow is said to be unsteady when the conditions and properties at any points change with time. The example of the unsteady flow is water being pumped through a fixed system at an increasing rate (Swarup, 2000).

1.4.2(b) Laminar and turbulent flows

In fluid mechanics, some flows are smooth and orderly while others are rather chaotic. The researchers distinguish the highly ordered fluid motion characterized by smooth layers of fluid as laminar flow. The word laminar comes from the movement of adjacent fluid particles together in “laminates”. For example, the flow of high viscosity fluids such as oils at low velocities is normally laminar. On the other hand, the highly disordered fluid motion is called the turbulent. For instance, the flow of low viscosity fluids at high velocities such as air is typically turbulent. In addition, the transition from laminar to turbulent flow does not occur suddenly; rather, it occurs over some region in which the flow fluctuates between laminar and turbulent flows before it becomes fully turbulent. A flow between the laminar and turbulent is called the transitional flow. The flow depends mostly on the ratio of inertial forces to viscous forces in the fluid. This ratio is called the Reynolds number and the expression is given by (Cengel & Cimbala, 2006)

$$Re = \frac{\text{inertial forces}}{\text{viscous forces}} = \frac{\bar{\rho} \bar{u}_m \bar{L}}{\bar{\mu}}, \quad (1.12)$$

where $\bar{\rho}$ is the density, \bar{u}_m is the mean velocity (average velocity), \bar{L} is the length of conduits and $\bar{\mu}$ is the fluid viscosity. The flow is laminar when $Re < 2300$, transitional when $2300 \leq Re \leq 4000$ and turbulent when $Re > 4000$. At a small and moderate Re , the flow is laminar as viscous forces are large enough to control the fluctuation of fluid and keep the velocity to be constant. While at large Re , the flow is turbulent as viscous force cannot control the rapid fluctuation of fluid (Cengel & Cimbala, 2006).

1.4.2(c) Incompressible and compressible flows

A flow is categorized as being compressible or incompressible, depending on the level of variation of density during flow. A flow is said to be incompressible if the density remains nearly constant throughout. Thus, the volume of every part of fluid remains unchanged over the course of its motion when the flow is incompressible (Cengel & Cimbala, 2006). Meanwhile, the flow is said to be compressible when the fluid changes with the density. In this study, the density of blood is essentially constant. Therefore, the incompressible flow will be considered in this present study.

1.4.2(d) Fully-developed flow

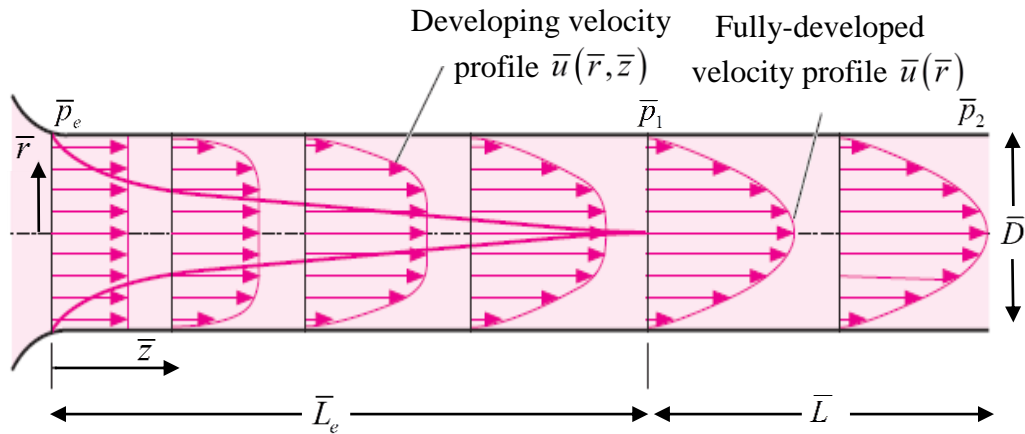


Figure 1.8: The development of velocity profile in a circular pipe (modified from Cengel & Cimbala, 2006).

Consider the steady flow of a fluid through a circular pipe. Figure 1.8 depicts the development of velocity profile in a circular pipe using a cylindrical coordinate system, where \bar{u} is the fluid velocity, \bar{p}_e is the pressure at the entrance region, \bar{p}_1 and \bar{p}_2 are the pressures at the fully developed region, \bar{L}_e is the entrance length, \bar{L} is the fully-developed length and \bar{D} is the diameter of a circular pipe. This figure shows two profiles, which are developing velocity and fully-developed velocity profiles. The flow is two-dimensional in the entrance region of a circular pipe since the velocity changes in both the \bar{r} and \bar{z} directions. Meanwhile, the flow is said to be a fully-developed and becomes one-dimensional when the velocity profile develops fully and remains unchanged after some distance from the inlet if the circular pipe is sufficiently long, where $\bar{L}_e \cong 0.05Re\bar{D}$ for laminar flow and $\bar{L}_e \cong 1.359Re^{1/4}\bar{D}$ for turbulent flow (Cengel & Cimbala, 2006). Since the velocity is varies in the radial \bar{r} direction but is the same at any axial \bar{z} direction and symmetric at any azimuthal angle $\bar{\psi}$ direction, thus, the velocity is assumed negligibly small in the $\bar{\psi}$ and \bar{z} directions (Cengel & Cimbala, 2006).

1.4.2(e) Plane Poiseuille flow

A plane Poiseuille flow or known as a channel flow is the flow between two stationary parallel flat plates, where the fluid is forced by pressure gradient in the \bar{z} direction. The plane Poiseuille flow occurs when the fluid flows from high pressure to low pressure, applying a shear stress on the walls in the direction of flow. The pressure gradient $d\bar{p}/d\bar{z}$ in plane Poiseuille flow is constant everywhere, where \bar{p} is the pressure of the fluid. Figure 1.9 shows the velocity profile $\bar{u}(\bar{x})$ of a plane Poiseuille flow, where \bar{h} is the semi-width of a channel, $d\bar{p}/d\bar{z}$ is the pressure gra-